Molecular and Biochemical Analyses of Platelet-Derived Growth Factor Receptor (PDGFR) B, PDGFRA, and KIT Receptors in Chordomas

Elena Tamborini,[1] Francesca Miselli,[1] Tiziana Negri,[1] M. Stefania Lagonigro,[1] Samantha Staurengo,[1] Gian Paolo Dagrada,[1] Silvia Stacchiotti,[2] Elisa Pastore,[1] Alessandro Gronchi,[2] Federica Perrone,[1] Antonino Carbone,[1] Marco A. Pierotti,[3] Paolo G. Casali,[2] and Silvana Pilotti[1]

Abstract

Purpose: We have previously shown the presence of an activated platelet-derived growth factor (PDGF) receptor (PDGFR) B and its ligand *PDGFB* in a limited number of patients with clinical and radiological responses to imatinib mesylate treatment. This article describes the results of comprehensive molecular/biochemical analyses of the three receptors targeted by the drug (PDGFRB, PDGFRA, and KIT) in a series of 31 chordoma patients.

Experimental Design: The presence and activation status of PDGFRB, PDGFRA, and KIT receptors were investigated by means of immunoprecipitation and Western blot analyses complemented by immunohistochemistry, their expression level was analyzed by means of real-time PCR, and the occurrence of activating point mutations was investigated by means of cDNA sequencing. The *PDGFB, PDGFA,* and stem cell factor cognate ligands were investigated by reverse transcription-PCR, and gene status was assessed by fluorescence *in situ* hybridization.

Results: The results show that PDGFRB was highly expressed and phosphorylated, whereas PDGFRA and KIT were less expressed but phosphorylated and thus activated. These findings, together with the absence of gain-of-function mutations and the presence of the cognate ligands, strongly support the hypothesis that the activation mechanism is the autocrine/paracrine loop. No role seems to be played by gene amplification.

Conclusions: In the light of our findings, the clinical benefit observed in chordoma patients treated with imatinib seems to be attributable to the switching off of all three receptors.

Chordomas are rare, low-grade neoplasms originating from remnants of the fetal nothocord that mainly affect the sacrum, skull base region and, in a minority of cases, the cervical and thoracolumbar vertebrae (1). Three histologic variants with different morphologies have been described: the conventional or classic type, the chondroid type, and the dedifferentiated type.

Classic cytogenetic studies define these tumors as complex sarcomas because they are generally characterized by complex karyotypes. The analyses published thus far have found that the most frequent event is the deletion of 1p, the location of the potential cancer susceptibility region of locus 1p36.31-1p36.13. The results of combined loss of heterozygosity and reverse transcription-PCR analyses have suggested that several genes, including *CASP9*, *EPH2A*, and *DVL1*, may play an oncosuppressing role and be involved in chordoma development (2). Finally, losses of 1p and 3p and gains of chromosomes 7, 20, 5q, and 12q have been reported based on comparative genomic hybridization studies (3).

In relation to cell cycle–controlling genes, an immunophenotype-based study has found an alteration in the G_1-S checkpoint, principally restricted to p53 overexpression (4).

Very little is known about receptor tyrosine kinase (RTK) activation, but their RTK expression could offer useful alternative therapeutic targets because, as it is well known that chordomas do not respond to radiotherapy or conventional chemotherapy, the standard treatment is surgery. It has in fact been recently found that Met and epidermal growth factor receptor are highly expressed especially in primary chordomas (5).

We have previously shown the presence of an activated platelet-derived growth factor (PDGF) receptor (PDGFR) B and its *PDGFB* ligand in some chordomas and reported that an albeit limited number of patients treated with imatinib mesylate (Gleevec, Novartis Pharma AG, Basel, Switzerland), an inhibitor of some RTKs, including KIT, PDGFRA, and PDGFRB, all showed clinical and radiological response

Authors' Affiliations: [1]Experimental Molecular Pathology, Department of Pathology, [2]Department of Medical/Surgical Oncology, and [3]Scientific Director, Fondazione IRCCS, Istituto Nazionale dei Tumori, Milan, Italy

Received 6/30/06; revised 9/13/06; accepted 9/21/06.

Grant support: Associazione Italiana per la Ricerca sul Cancro 2004 and Italian Ministry of Health (Ricerca Finalizzata 2004).

The costs of publication of this article were defrayed in part by the payment of page charges. This article must therefore be hereby marked *advertisement* in accordance with 18 U.S.C. Section 1734 solely to indicate this fact.

Note: E. Tamborini and F. Miselli contributed equally to this work. P.G. Casali and S. Pilotti are senior coauthors.

Requests for reprints: Silvana Pilotti, Unit of Experimental Molecular Pathology, Department of Pathology, Istituto Nazionale per lo Studio e la Cura dei Tumori, Via G. Venezian 1, 20133 Milan, Italy. Phone: 39-02-23902260; Fax: 39-02-23902877; E-mail: silvana.pilotti@istitutotumori.mi.it.

doi:10.1158/1078-0432.CCR-06-1584

improvements and experienced an improvement in their quality of life (6).

In this study, we extended our analyses to all of the receptors targeted by imatinib mesylate in a series of 31 patients with conventional chordomas by investigating the presence and activation status of PDGFRB, PDGFRA, and KIT by means of immunoprecipitation and Western blot analyses complemented by immunohistochemistry. Their expression level was analyzed by real-time PCR, the presence of activating point mutations was investigated by means of cDNA sequencing, and the presence of the *PDGFB*, *PDGFA*, and stem cell factor *(SCF)* cognate ligands was investigated by means of reverse transcription-PCR. As gene amplification may also be one of the mechanisms responsible for receptor activation, gene status was assessed by means of fluorescence *in situ* hybridization (FISH).

The results showed that PDGFRB, PDGFRA, and KIT were all expressed and phosphorylated even if with different level of expression as shown also by quantitative analysis on their mRNAs. Together with the absence of gain-of-function mutations and the presence of the cognate ligands, these findings strongly support that the activation mechanism is the autocrine/paracrine loop. Gene amplification did not seem to play any role.

Materials and Methods

Patients and materials

We studied 31 chordomas affecting 19 males and 12 females with a median age of 59 years (23 primary tumors and 8 recurrences: 3 involving the clivus, 5 the vertebrae, and 23 the sacrum) by analyzing 20 frozen surgical specimens (15 in-house and 5 consultation cases), 8 frozen small biopsy specimens (6 in-house and 2 consultation cases), and 3 specimens in paraffin-embedded blocks (all consultation cases). All of the specimens used for the molecular/biochemical analyses had been excised before imatinib treatment. Eleven of the patients had undergone standard chemotherapy and/or radiotherapy (Table 1). Written informed consent was obtained from all the patients.

All the biochemical and molecular analyses were done on tissue sections carefully evaluated by the pathologist in terms of presence of normal tissues or necrosis.

Biochemical analysis

Positive and negative controls. A synovial sarcoma (7) and the 2N5A cell line (derived from the NIH3T3 cell line expressing the COL1-PDGFB fusion characterizing dermatofibrosarcoma protuberans; kindly provided by Dr. A. Greco, Department of Experimental Oncology, Fondazione IRCCS Istituto Nazionale Tumori, Milan, Italy) were used as positive controls for the PDGFRB blots; a gastrointestinal stromal tumor (GIST; tested molecularly) and the NIH3T3 cell line (American Type Culture Collection, Manassas, VA) were used for the PDGFRA protein expression/phosphorylation experiments; and a GIST (tested molecularly) plus the KIT/Δ559 cell line (8) overexpressing an activated KIT receptor were used in the KIT experiments. A pool of normal mesenchymal tissues (muscles, vessels, adipose tissue, and nerves) was used as a negative control of receptor expression levels.

Protein extraction and immunoprecipitation/Western blotting. The proteins were extracted, immunoprecipitated for PDGFRB, PDGFRA, and KIT, and blotted as described previously (9).

Immunohistochemistry

A representative paraffin block of formalin-fixed tumoral tissue from each patient was selected and phenotyped by means of immunoperoxidase analysis as described previously (9).

Table 1. Clinical features of chordoma patients

Case	Sex	Age	Site	Sample type	Material	Type
1	M	61	Sacrum	Primary	Frozen	Surgical specimen
2	M	25	Sacrum	Primary	Frozen	Surgical specimen
3	M	58	Sacrum	Primary	Frozen	Biopsy
4	F	64	Vertebrae	Primary	Frozen	Surgical specimen
5	F	65	Vertebrae	Primary	Frozen	Surgical specimen
6	F	66	Sacrum	Recurrent	Frozen	Biopsy
7	M	52	Sacrum	Primary	Frozen	Biopsy
8	M	61	Sacrum	Primary	Frozen	Biopsy
9	F	73	Sacrum	Primary	Frozen	Surgical specimen
10	M	57	Clivus	Primary	Frozen	Biopsy
11	F	28	Clivus	Primary	Frozen	Surgical specimen
12	F	60	Vertebrae	Primary	Frozen	Biopsy
13	M	58	Sacrum	Primary	Frozen	Surgical specimen
14	M	56	Sacrum	Primary	Frozen	Surgical specimen
15	M	70	Sacrum	Recurrent	Frozen	Biopsy
16	M	24	Clivus	Recurrent	Frozen	Surgical specimen
17	M	41	Sacrum	Recurrent	Frozen	Surgical specimen
18	M	49	Sacrum	Primary	Frozen	Surgical specimen
19	F	47	Sacrum	Recurrent	Frozen	Surgical specimen
20	M	66	Sacrum	Primary	Frozen	Surgical specimen
21	M	77	Sacrum	Primary	Frozen	Surgical specimen
22	M	59	Sacrum	Primary	Frozen	Surgical specimen
23	M	66	Sacrum	Primary	Frozen	Surgical specimen
24	F	65	Sacrum	Recurrent	Frozen	Surgical specimen
25	F	60	Sacrum	Primary	Frozen	Surgical specimen
26	M	75	Sacrum	Primary	Frozen	Surgical specimen
27	F	41	Sacrum	Recurrent	Frozen	Biopsy
28	M	69	Vertebrae	Primary	Frozen	Surgical specimen
29	F	59	Sacrum	Primary	Paraffin	—
30	M	51	Vertebrae	Recurrent	Paraffin	—
31	F	66	Sacrum	Primary	Paraffin	—

RNA extraction, reverse-transcription PCR, sequencing analysis, and ligand assessment

Total RNA was extracted from freshly frozen tissue and reverse transcribed as described previously (7). The obtained cDNA was amplified using specific primer pairs for *PDGFRA*, *PDGFRB*, and *c-KIT* genes as listed in a previous publication (9). The same cDNAs were used to detect the presence of *PDGFA, PDGFB, and SCF* ligands as already reported (9).

Fluorescence *in situ* hybridization

Cytologic specimens and touch imprints. The slides were placed under running water for a few seconds, air dried, and then fixed as reported by Lagonigro et al. (9). The FISH probes were bacterial artificial chromosome clones RP11-231C18 (*PDGFRA* gene, 4q12), RP11-368O19 (*PDGFRB* gene, 5q31-32), and RP11-586A2 (*c-Kit* gene, 4q12), all of which were kindly provided by Dr. M. Rocchi (Resources for Molecular Cytogenetics, University of Bari, Bari, Italy).

Tissue sections. The same probe mixtures were used on 5-μm thin sections as described previously (9).

Detection and relative quantification of receptor expression

PDGFRB, *PDGFRA*, and *c-Kit* cDNAs were relatively quantified by means of real-time quantitative PCR (ABI PRISM 5700 PCR Sequence Detection Systems, Applied Biosystems, Foster City, CA) using a Taqman-based analysis. Each reaction contained 1× Taqman Universal Master Mix (Applied Biosystems), 1 μL of template cDNA, 0.9 μmol/L of each forward and reverse primer, and 0.2 μmol/L of the fluorogenic Taqman probes in a total volume of 25 μL. Cycling was started with 2 minutes at 50°C and 10 minutes at 95°C followed by 40 cycles of 15 seconds at 95°C and 1 minute at 60°C. All of the experiments were done in triplicate.

hRNaseP and glyceraldehyde-3-phosphate dehydrogenase, which were detected by means of a commercially available kit (Applied Biosystems), were used as internal controls. To assess the amplification efficiency of receptors and controls, we made standard curves using serial cDNA dilutions.

The $2^{-\Delta\Delta Ct}$ method (10) was used to calculate the relative changes in receptor gene expression determined by means of real-time quantitative PCR experiments: $\Delta\Delta C_t$ = [ΔC_t (unknown sample) − ΔC_t (calibrator sample)] = [C_tGI (unknown sample) − C_tGR (unknown sample)] − [C_tGI (calibrator sample) − C_tGR (calibrator sample)], where GI is the gene of interest, GR is the gene reference, and the calibrator is the sample chosen to represent 1× expression of the gene of interest. The calibrator sample was represented by a pool of normal mesenchymal tissues (muscles, vessels, adipose tissue, and nerves).

Each amplification was done using a positive control of reaction represented for *c-Kit* by seven GISTs that had previously been characterized as overexpressing KIT protein in immunohistochemistry and immunoprecipitation/Western blot experiments; for *PDGFRA*, a GIST carrying the D842V mutation in *PDGFRA* already shown to overexpress this receptor; for *PDGFRB*, a chondrosarcoma already shown to be positive for this receptor.

Results

Biochemical analysis

All of the samples with sufficient frozen material (Table 2) were analyzed by means of immunoprecipitation and Western blot experiments to assess the expression and status of the PDGFRB, PDGFRA, and KIT receptors.

Platelet-derived growth factor receptor B. Eighteen samples (15 in-house and 1 consultation surgical specimens and 2 in-house small biopsy specimens) were investigated by immunoprecipitating equal amounts of total protein extracts. Membrane incubation with an anti-phosphotyrosine antibody revealed a 180-kDa band corresponding to an activated receptor in all of the samples. Figure 1A shows eight representative cases; in some of which, the band was more intense. Receptor expression was revealed by incubating the membrane with an anti-PDGFRB antibody and proved to be comparable in all of the samples although less intense in some. PDGFRB expression was greater in all of the analyzed chordomas than in the synovial sarcoma specimen used as positive control.

Table 2. Summary of RTK biochemical data and relative quantification by quantitative real-time PCR for the corresponding mRNAs with respect to a normal tissue pool

Case	Protein									mRNA		
	PDGFRB			PDGFRA			KIT			*PDGFRB* ($2^{-\Delta\Delta Ct}$)	*PDGFRA* ($2^{-\Delta\Delta Ct}$)	*c-Kit* ($2^{-\Delta\Delta Ct}$)
	Expr	Phosph	IHC	Expr	Phosph	IHC	Expr	Phosph	IHC			
1	+	P								8×10^{-1}	2×10^{-1}	2×10^{-1}
2	+	P	+			+			−	5×10^{-1}	2×10^{-1}	2×10^{-2}
3			+			+			−	2.5	4×10^{-1}	3
4	+	P		+	P		+	P		6×10^{-1}	6×10^{-2}	3×10^{-1}
5	+	P		+	P		+	P		6×10^{-1}	3×10^{-1}	2×10^{-1}
6	+	P					−			NE	NE	NE
7			+			+	−		−	10.5	2	NE
8			+			+			+	NE	1.2	3×10^{-1}
9	++	P								5	5×10^{-1}	4
10										NE	NE	NE
11			+			+			−	15.6	1.8	8×10^{-1}
12										NE	NE	NE
13	+	P	+			+			−	4×10^{-1}	2×10^{-1}	6×10^{-1}
14										6×10^{-1}	1×10^{-1}	4×10^{-1}
15	+	P	+			+			−	NE	NE	NE
16			+			+			−	3	1	1
17	++	P	+	+	P	+	+	P	−	1.4	1.2	2
18	+	P	+	+	P	+	+	P	−	NE	3	1.6
19	++	P	+	+	P	+	+	P	−	1.4	1.2	2×10^{-1}
20	+	P	+	+	P	+	+	P	−	3×10^{-1}	1×10^{-1}	1×10^{-1}
21	+	P	+	+	P	+	+	P	−	2.5×10^{-1}	1×10^{-1}	8×10^{-2}
22	++	P	+	+	P	+	+	P	−	1	1×10^{-1}	5×10^{-2}
23	++	P	+	+	P	+	+	P	−	1.3	3×10^{-1}	2×10^{-1}
24	+	P	+	+	P	+	+	P	−	3×10^{-1}	1×10^{-2}	4×10^{-2}
25	+	P	+	+	P	+	+	P	−	5×10^{-1}	4×10^{-1}	3×10^{-1}
26	+	P	+	+	P	+	+	P	−	2.5×10^{-1}	3×10^{-1}	1×10^{-1}
27										NE	2	1.2
28										NE	NE	NE
29										NE	NE	NE
30										NE	NE	NE
31										NE	NE	NE
								Median value		2.34	0.7	0.7

NOTE: The values reported on mRNAs are expressed as fold expression compared with normal tissue pool.
Abbreviations: Expr, receptor expression; Phosph, receptor phosphorylation and thus activation; IHC, immunohistochemical analysis; NE, not evaluable.

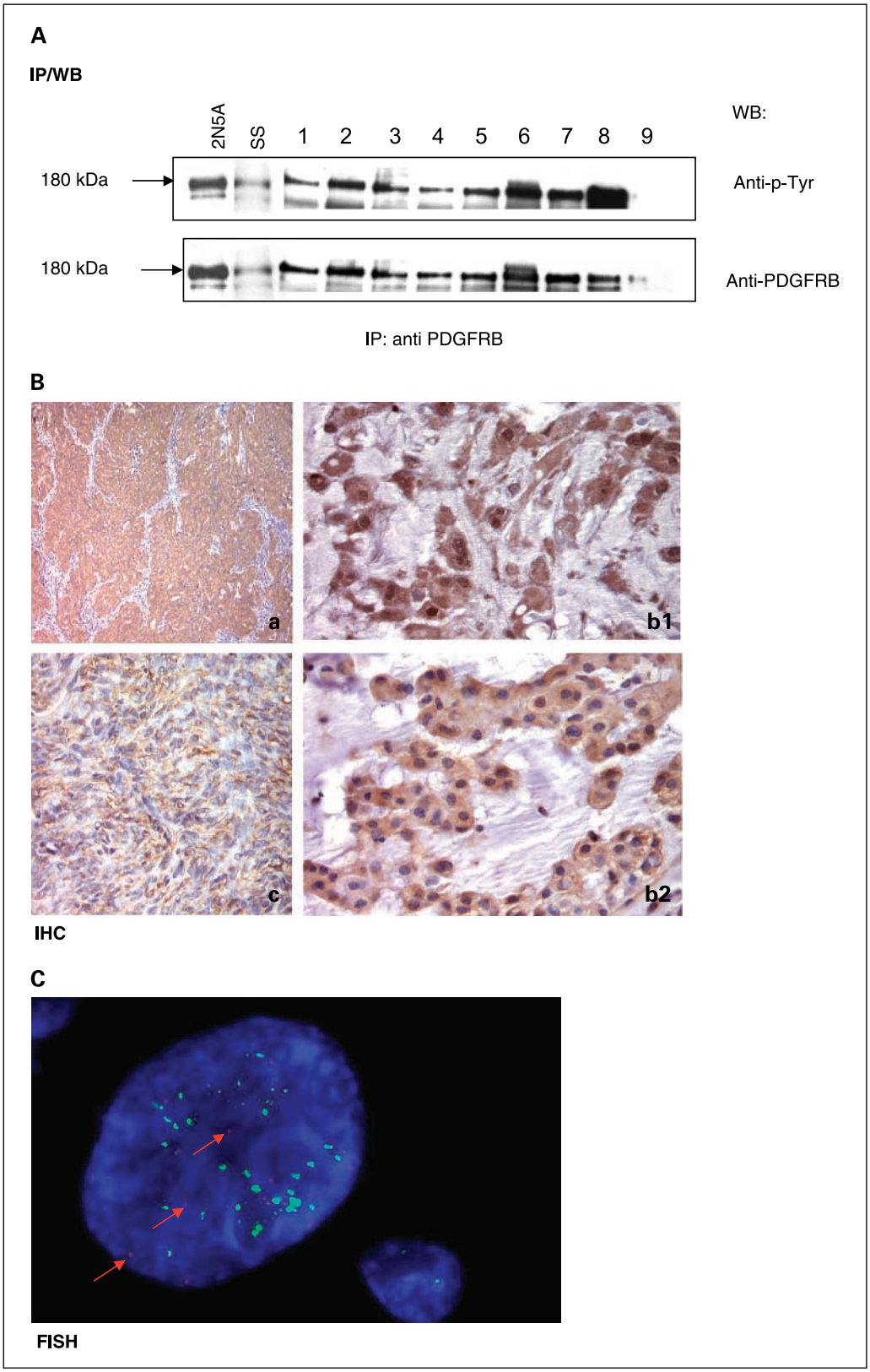

Fig. 1. PDGFRB expression. *A,* immunoprecipitation (*IP*) and Western blot (*WB*) analysis. For each sample, 1 mg of total protein extract was immunoprecipitated using anti-PDGFRB antibody, run on gel, and blotted with the indicated antibodies. As positive controls, a 2N5A cell line and a synovial sarcoma (*SS*) specimen were used. Lanes 1 to 7, seven representative cases; lane 8, chondrosarcoma already shown positive for this receptor; lane 9, pool of normal tissues is reported. *B,* immunohistochemical (*IHC*) expression. Cytoplasmic decoration in chordoma (*b1* and *b2*) using the Santa Cruz Biotechnology (Santa Cruz, CA) antibody on paraffin-embedded material (3,3′-diaminobenzidine). As positive controls, a synovial sarcoma (*a*) and dermatofibrosarcoma protuberans (*c*) were used. *C,* FISH analysis. Left, amplification of *PDGFRB* (spectrum green) in the nucleus; right, condition of disomy. Red arrows, some signals of a probe specific for a 5p region.

Platelet-derived growth factor receptor A. PDGFRA was investigated in 12 samples, all of which were in-house surgical specimens that showed a band corresponding to the activated receptor. Incubation with the anti-PDGFRA antibody used to detect its level of expression revealed a band of 170 kDa in all of the samples, and comparison with the GIST used as a positive control indicated that chordomas express less PDGFRA (Fig. 2A).

KIT. Total protein extracts derived from 14 samples (12 in-house surgical specimens and 2 biopsies) were immunoprecipitated using an antibody specific for the KIT receptor, 12 of which showed a 145-kDa phosphorylated band after membrane incubation with an anti-phosphotyrosine antibody. Incubation of the same membranes with an anti-KIT antibody revealed a 145-kDa band corresponding to the KIT receptor. Figure 3A shows that the level of expression was at least 10 times lower than that found in the positive controls (the Δ559 cell line and a GIST). Two samples were negative.

Immunohistochemical analysis

Immunohistochemical analysis was based on paraffin-embedded specimens from 18 of the 21 in-house cases: 15 surgical specimens and 3 small biopsies (the remaining 3 were not representative). All of the sections obtained from a representative block of each case screened for PDGFRB proved to be positive with cytoplasm reactivity, which was more intense than in the positive control (synovial sarcoma, chondrosarcoma, and dermatofibrosarcoma protuberans; data not shown; Fig. 1B); they were also PDGFRA positive and the

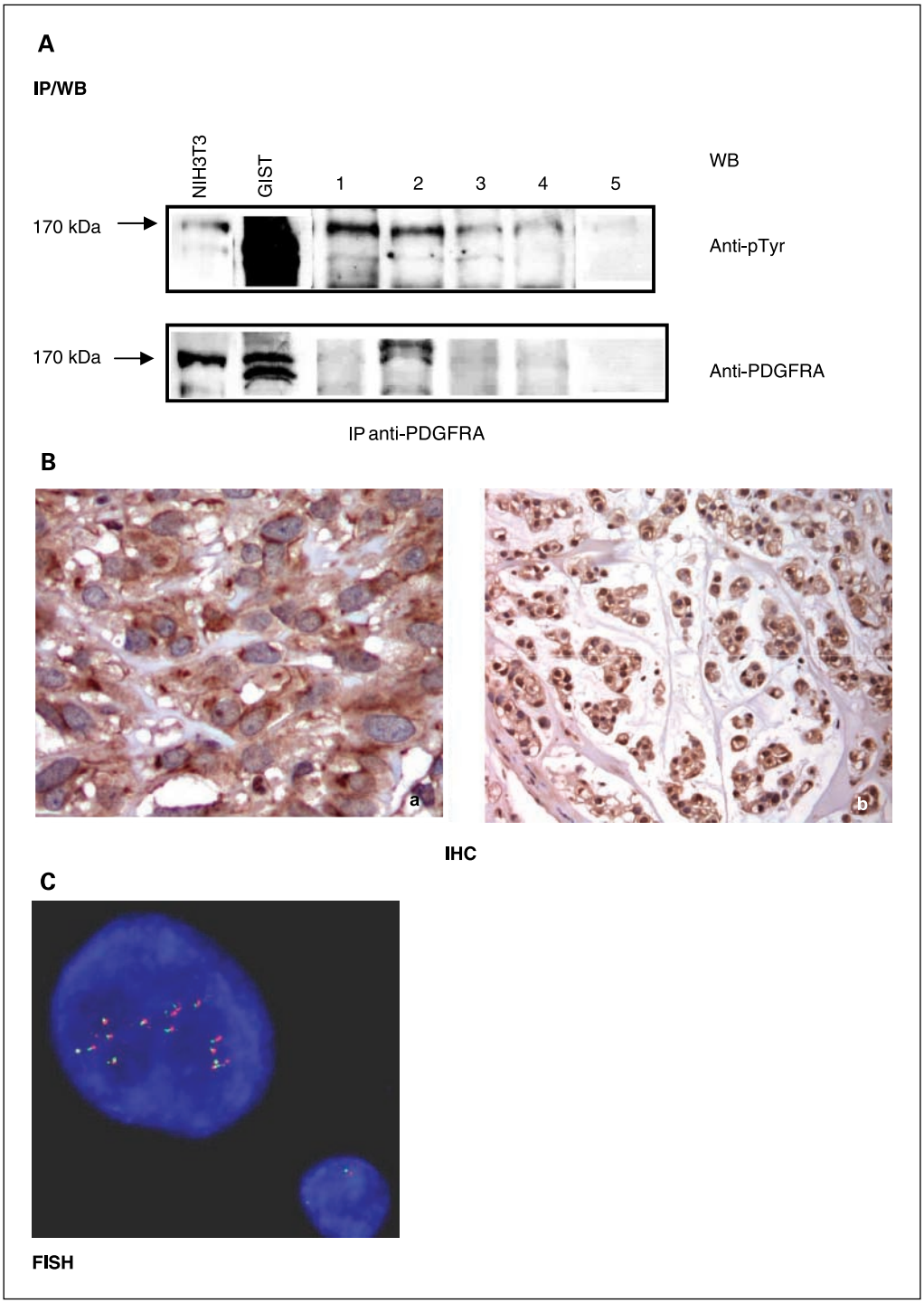

Fig. 2. PDGFRA expression. *A,* immunoprecipitation and Western blot analysis. For each sample, 1 mg of total protein extract was immunoprecipitated using anti-PDGFRA antibody, run on gel, and blotted with the indicated antibodies. As positive control, the NIH3T3 cell line and a mutated in exon 18 (D842V) PDGFRA GIST were used. Lanes 1 to 4, four representative cases; lane 5, pool of normal tissues is reported. *B,* immunohistochemical expression. *a,* the same GIST case used as positive control in (*A*). *b,* cytoplasmic decoration using the Santa Cruz Biotechnology antibody on paraffin-embedded material (3,3′-diaminobenzidine) on a representative case. *C,* FISH analysis. Left, amplification of *PDGFRA* (spectrum orange) and *c-Kit* (spectrum green) in the nucleus; right, condition of monosomy.

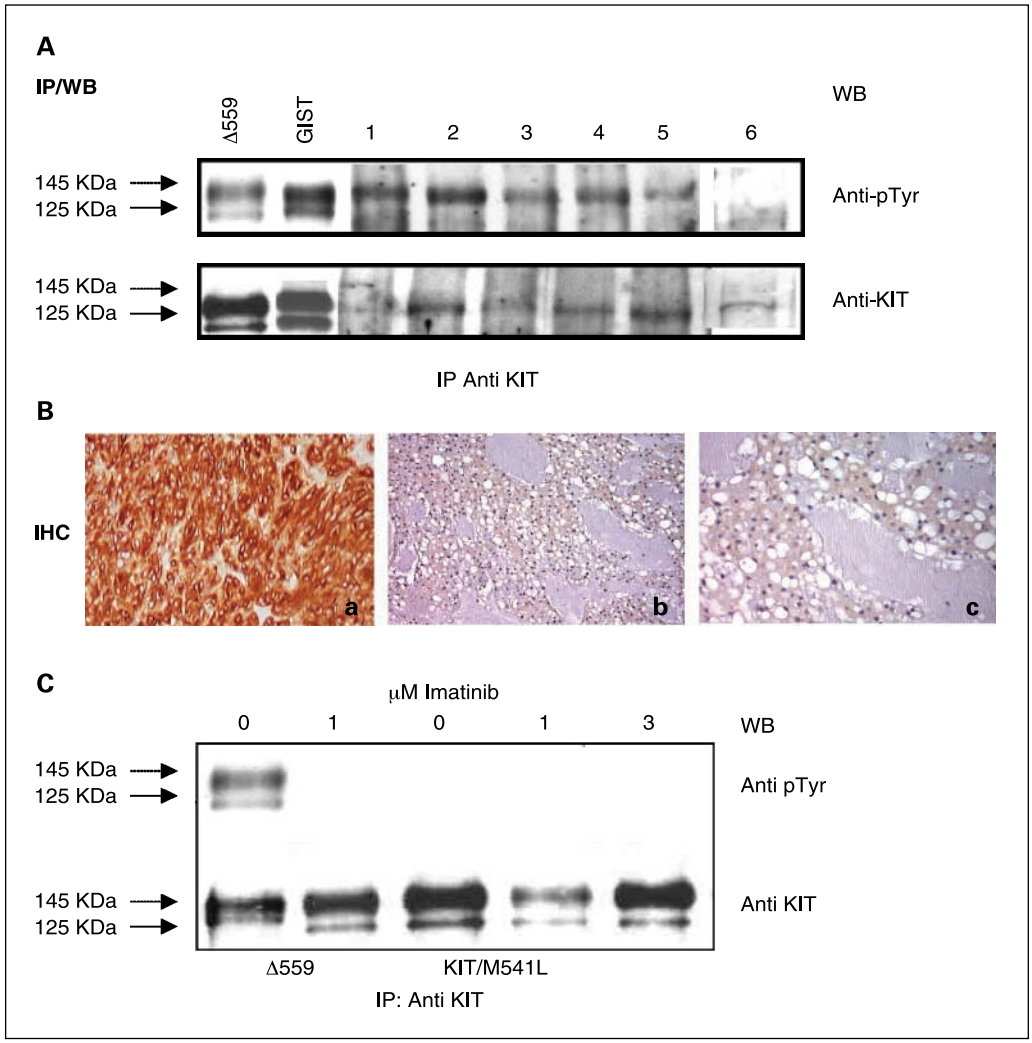

Fig. 3. KIT expression. *A,* immunoprecipitation and Western blot analysis. For each sample, 1 mg of total protein extract was immunoprecipitated using anti-KIT antibody, run on gel, and blotted with the indicated antibodies. As positive control, the Δ559 cell line (carrying a mutation in exon 11 of *c-Kit*) and a mutated *c-Kit* GIST were used. Lanes 1 to 5, five representative cases; lane 6, pool of normal tissues is reported. *B,* immunohistochemical expression. Case 8 (*b* and *c*, higher resolution) resulted to be very slight immunoreactive compared with a positive CD117 GIST (*a*). *C,* COS1 cells were transiently transfected with the *c-Kit* constructs (KIT/Δ559 and KIT/M541L) and were incubated with imatinib at the indicated doses for 8 hours. Immunoprecipitation/Western blot experiments were done as described in (*A*).

staining was once again cytoplasmatic (Fig. 2B). One case (case 20) was not evaluable.

The same samples were incubated with CD117 antibody: no staining was observed in 17, and the remaining sample (case 8) was only slightly positive. The mast cells used as positive in-built controls were highly immunoreactive in all of the samples.

Detection and relative quantification of *PDGFRB*, *PDGFRA*, and *c-Kit* expression

PDGFRB, *PDGFRA*, and *c-Kit* mRNAs were relatively quantified by means of real-time quantitative PCR.

The standard receptors and control curves (hRNaseP and glyceraldehyde-3-phosphate dehydrogenase) of the serial cDNA dilutions showed that ΔC_t did not change with template dilution, thus indicating that the target and reference amplification efficiencies were very similar (data not shown).

We relatively quantified receptor expression in 23 chordomas (the 3 paraffin-embedded samples were excluded, as were 5 other samples with no more cDNA) using the $2^{-\Delta\Delta Ct}$ method; the calibrator sample was the average ΔC_t obtained from a pool of normal mesenchymal tissues and thus expressing a basal level of receptor mRNAs arbitrarily indicated as 1. In Table 2, all the values are reported as fold expression compared with normal tissue pool.

The median value $2^{-\Delta\Delta Ct}$ for *PDGFRB* was 2.34, indicating that chordomas express this receptor more than the pool of normal tissues. By contrast, the median values $2^{-\Delta\Delta Ct}$ of 0.7 for *PDGFRA* and *c-KIT* indicate that this tumor histotype expresses less mRNA than the calibrator sample.

PDGFRB, *PDGFRA*, and *c-KIT* mutational screening

To exclude the presence of gain-of-function mutations as the cause of the receptor activation observed in the immunoprecipitation/Western blot experiments, the cDNAs of all the samples were sequenced. The cDNAs obtained from frozen material (28 cases) allowed us to sequence the cDNA receptors from the transmembrane domain to the COOH terminus (exons 10-20 for *PDGFRB*, exons 10-22 for *PDGFRA*, and exons 8-21 for *c-KIT*); in the three cases for which only paraffin-embedded material was available, the sequencing was restricted to the exons that are hotspots of mutations (exons 9, 11, 13, and 17 for *c-KIT*; exons 12 and 18 for *PDGFRA;* and none for *PDGFRB*). The results are summarized in Table 3.

Platelet-derived growth factor receptor B. No amino acid substitutions were found, but there were several silent mutations: G2210A (cases 11 and 20), C2441A (case 15), G2840A (case 8), and A2957G (cases 6, 8, 9, 10, 11, 15, 17, 19, 20, 21, 23, 24, and 26).

Table 3. Summary of the sequencing data and reverse transcription-PCR on the cognate ligands

Case	*PDGFRB*	*PDGFB*	*PDGFRA*	*PDGFA*	*c-Kit*	*SCF*
1	wt	+	S478P, G2203A, C2866T	+	wt	L/S
2	wt	+	wt	+	C2394T	L/S
3	wt	+	C2866T	+	M541L, G2586C	L
4	wt	+	wt	+	M541L	L/S
5	wt	+	wt	+	M541L	L/S
6	A2957G	+	wt	+	M541L	L/S
7	wt	+	wt	+	M541L	L
8	G2840A, A2957G	+	wt	+	wt	L/S
9	A2957G	+	wt	+	M541L	L/S
10	A2957G	+	wt	+	wt	L/S
11	G2210A, A2957G	+	wt	+	wt	L/S
12	wt	+	wt	+	M541L	L/S
13	wt	+	wt	+	A1638G	L/S
14	wt	+	wt	+	wt	L/S
15	C2441A, A2957G	+	S478P, G2203A, C2866T	+	A1638G	L/S
16	wt	+	wt	+	wt	L/S
17	A2957G	+	wt	+	wt	L/S
18	wt	+	wt	+	wt	L/S
19	A2957G	+	S478P, G2203A, C2866T	+	wt	L/S
20	G2210A, A2957G	+	wt	+	wt	L/S
21	A2957G	+	wt	+	wt	L/S
22	wt	+	S478P, G2203A, C2866T	+	M541L	L/S
23	A2957G	+	wt	+	M541L	L/S
24	A2957G	+	wt	+	wt	L/S
25	wt	+	wt	+	M541L, G2586C	L/S
26	A2957G	+	wt	+	wt	L/S
27	wt	+	wt	+	C2394T	L/S
28	wt	+	wt	+	C2394T	L/S
29	wt	+	wt	+	wt	—
30	NE	+	NE	+	M541L	—
31	NE	+	G2203A, C2866T	+	wt	—

Abbreviations: wt, wild-type; L, soluble SCF; S, membrane-bound SCF.

Platelet-derived growth factor receptor A. The S478P polymorphism was detected in four patients (1, 15, 19, and 22). The observed silent mutations were G2203A (cases 1, 15, 19, 22, and 31) and C2866T (cases 1, 3, 15, 19, 22, and 31). In brief, no activating point mutations were found.

c-Kit. All of the cases showed alternative splicings of exons 9 and 15, and 11 (34%) showed the previously described exon 10 mutation responsible for the M541L substitution. The silent mutations were A1638G (cases 13 and 15), C2394T (cases 2, 27, and 28), and G2586C (cases 3 and 25), but no activating point mutations were found.

Biochemical characterization of KIT/M541L receptor. Given the frequency of the exon 10 mutation in our chordoma patients, we used site-directed mutagenesis to introduce M541L substitution into a wild-type KIT-expressing vector and transiently transfected COS1 cells to assess the role of M541L in KIT activation and, therefore, imatinib response. Immunoprecipitation/Western blot experiments using total cell extracts and an anti-phosphotyrosine antibody showed that KIT/M541L receptors are poorly phosphorylated compared with the positive control used in the same experiment (KIT/Δ559; Fig. 3C). We therefore concluded that this mutation is not activating and that imatinib has no effect on it.

Ligand expression

To verify whether receptor activation was due to the presence of an autocrine/paracrine loop, we investigated the cognate ligands of each receptor in all 31 cases.

PDGFB and PDGFA. The cDNAs were analyzed by means of reverse transcription-PCR, and all of the samples were positive for both ligands.

Stem cell factor. The KIT cognate ligand *SCF* was detected in all but three samples (cases 29, 30, and 31, in which the lack of amplification was probably due to the poor quality of the template). Almost all of the positive cases expressed both forms (corresponding to soluble and membrane-bound *SCF*), but two (cases 3 and 7) showed only the soluble *SCF* isoform.

FISH analysis

Gene copy numbers were investigated by FISH, with a complete analysis of all three receptors being made using 14 adequate touch imprints obtained from frozen specimens by means of apposition on precleaned slides. Eleven cases were characterized by a normal disomic hybridization pattern, with 1 (case 4) showing monosomic nuclei and another (case 26) showing a substantial number of tetrasomic cells. Of the remaining three cases, case 3 had tetraploid cells associated with a hemizygous deletion of chromosome 5 in which *PDGFRB* is located, case 17 showed chromosome 5 polysomy/amplification in a disomic/monosomic condition, and case 22 showed polysomy/amplification for chromosomes 4 (where *c-Kit* and *PDGFRA* are located) and 5 (Figs. 2C and 1C, respectively).

The cases with more than two signals per cell (cases 17, 22, and 26) were further analyzed using tissue sections from frozen samples, which confirmed the apposition data.

Discussion

In a previous study of a limited series of patients responding to imatinib (6), we found that chordomas express both activated PDGFRB and its *PDGFB* cognate ligand, a finding that led us to hypothesize that the activation mechanism may be an autocrine/paracrine loop. For the purposes of the present retrospective study of a larger number of patients, we extended the analysis to include PDGFRA and KIT, the other two RTKs that are known to respond to imatinib. Immunoprecipitation/Western blot experiments were done in all of the cases for which cryopreserved material was available, and FISH experiments were done in 14 cases; all of the cases underwent cognate ligand detection and gene sequencing as well as mRNA quantification of each receptor.

PDGFRB expression and evidence of receptor phosphorylation were detected in all of the 18 samples analyzed; PDGFRB expression varied from sample to sample but was generally higher than in the synovial sarcoma specimens used as positive controls (7) and comparable with chondrosarcomas. Interestingly, the cases identified as ++ in Table 2 were shown to have a higher mRNA expression level (cases 9, 17, 19, 22, and 23) with respect to the cases identified as +. However, a discrepancy between mRNA and protein expression is present as shown by cases with lower mRNA level but expressing PDGFRB more than the pool. Unfortunately, the low number of cases analyzed does not permit to draw a conclusion between mRNA and protein expression. In line with the high biochemical expression levels, immunostaining was more intense than in the dermatofibrosarcoma protuberans used as a reference (11).

To confirm the presence of an autocrine/paracrine loop, we sequenced the gene from the transmembrane domain to the COOH terminus of *PDGFRB* in a search for activating point mutations, although no alterations in this receptor have been previously reported. We did not find any alterations causing amino acid changes. Together with the presence of the cognate ligand *PDGFB* and of wild-type receptors, this finding strongly supports the hypothesis that activation is sustained by an autocrine loop, although the occurrence of gene amplification in a limited number of cases suggests that other mechanisms may be responsible for the PDGFRB deregulation in chordoma.

The same approach was applied to PDGFRA and KIT, the expression and activation status of which were investigated by means of immunoprecipitation experiments. PDGFRA proved to be less expressed and phosphorylated when compared with a GIST patient whose genotyping indicated a mutated gene (D842V in exon 18), but its expression level was comparable with the one present in a pool of normal tissues in which, however, PDGFRA was not activated. Similarly, the expression of KIT was lower than that observed in a patient with GIST carrying an exon 11 mutation but comparable with the one detected in the pool. KIT activation was present in chordomas but not in the pool. These findings correlated with real-time experiments for both *c-Kit* and *PDGFRA* mRNAs, resulting less expressed than the positive controls (data not shown) but comparable with the values detected in the normal pool. All of these findings, in addition to the detection of *PDGFA* and *SCF* ligands and the absence of activating point mutations affecting the coding region, suggest that these two receptors are also activated by an autocrine/paracrine loop.

Surprisingly, an M541L amino acid substitution in KIT was found in 34% of the patients, but transfection experiments using KIT/M541L-expressing COS1 cells treated with imatinib showed that this substitution is not activating.

At this stage, we can say that chordomas show a deregulated expression and activation pattern of PDGFRB, PDGFRA, and KIT and that this may be inhibited by imatinib. The role of this RTK expression/activation pattern in maintaining a malignant phenotype seems to be different from that of KIT deregulation in GIST. Given the absence of the pivotal role of KIT activating mutations and the constitutive pathologic activation of wild-type imatinib-related receptors in chordoma, it is possible that more effective tumor inhibition could be achieved by means of multitarget anti-tyrosine kinase treatments. These different mechanisms of activation and, consequently, inhibition may explain why chordomas respond more slowly to imatinib than GISTs (6).[4]

About the observation that changes in tumor tissue are more important than changes in tumor size,[5] two points need to be underlined. Firstly, our experience with post-imatinib treated tumors is currently restricted to biopsy material, a possibly misleading window. Secondly, chordoma is a bone (not a soft tissue) tumor whose compactness is due to its rigid, mineralized extracellular matrix. Consequently, even if the two types of tumor share similar tissue changes, the presence of a tumor scaffold in chordomas cannot allow the tumor shrinkage frequently observed in GISTs.

Although other factors may also be involved in the similarities and differences between chordomas and GISTs, our data seem to provide one explanation as to why imatinib has some degree of antitumor activity in this rare disease (i.e., the existence of an autocrine/paracrine loop involving some imatinib-related RTKs). A similar gene profile has been recently reported in chondrosarcomas (9), and the amplification of *PDGFRA* and *c-KIT* has been described in malignant peripheral nerve sheath tumors (12), thus widening the spectrum of tumors that may benefit from treatment with RTK inhibitors.

[4] P.G. Casali, submitted for publication.
[5] P. Casali, S. Stacchiotti, A. Messina, et al. Unpublished data.

References

1. Heffelfinger MJ, Dahlin DC, MacCarty CS, et al. Chordomas and cartilaginous tumors at the skull case. Cancer 1973;32:410–20.
2. Riva P, Crosti F, Orzan F, et al. Mapping of candidate region for chordoma development to 1p36.13 by LOH analysis. Int J Cancer 2003;107:493–7.
3. Brandal P, Bjerkehagen B, Danielsen H, et al. Chromosome 7 abnormalities are common in chordomas. Cancer Genet Cytogenet 2005;160:15–21.
4. Naka T, Boltze C, Kuester D, et al. Alteration of G_1-S checkpoint in chordoma. Cancer 2005;104:1255–63.

5. Weinberg PM, Yu Z, Kowalski D, et al. Differential expression of epidermal growth factor receptor, c-Met, and Her2/neu in chordoma compared with 17 other malignancies. Arch Otolaryngol Head Neck Surg 2005;131:707–11.

6. Casali P, Messina A, Stacchiotti S, et al. Imatinib mesylate in chordoma. Cancer 2004;101:2086–97.

7. Tamborini E, Bonadiman L, Greco A, et al. Expression of ligand-activated KIT and PDGFRβ tyrosine kinase receptors in synovial sarcoma. Clin Cancer Res 2004; 10:938–43.

8. Tamborini E, Bonadiman L, Greco A, et al. A new mutation in KIT receptor ATP pocket is responsible for acquired resistance to imatinib in a patient with gastrointestinal stromal tumor. Gastroenterology 2004;127:294–9.

9. Lagonigro MS, Tamborini E, Negri T, et al. PDGFRα, PDGFRβ, and KIT expression/activation in conventional chondrosarcoma. J Pathol 2006;208:615–23.

10. Winer J, Jung CK, Shackel I, et al. Development and validation of real-time quantitative reverse transcriptase-polymerase chain reaction for monitoring gene expression in cardiac myocytes *in vitro*. Anal Biochem 1999;270:41–9.

11. McArthur GA, Demetri GD, van Oosterom A, et al. Molecular and clinical analysis of locally advanced dermatofibrosarcoma protuberans treated with imatinib: Imatinib Target Exploration Consortium Study B2225. J Clin Oncol 2005;23:866–73.

12. Holtkamp N, Okuducu AF, Mucha J, et al. PDGFRA and KIT dysregulation and mutation in malignant peripheral nerve sheath tumours. Carcinogenesis 2006;27:664–71.